Bio-Design and Manufacturing (2021) 4:526–540
https://doi.org/10.1007/s42242-021-00134-7

REVIEW

3D tumor model biofabrication

Ming Li[1] · Xueer Song[1] · Sha Jin[1] · Kaiming Ye[1]

Received: 24 October 2020 / Accepted: 5 April 2021 / Published online: 4 May 2021

Abstract

Animal models have been extensively used in cancer pathology studies and drug discovery. These models, however, fail to reflect the complex human tumor microenvironment and do not allow for high-throughput drug screening in more human-like physiological conditions. Three-dimensional (3D) cancer models present an alternative to automated high-throughput cancer drug discovery and oncology. In this review, we highlight recent technology innovations in building 3D tumor models that simulate the complex human tumor microenvironment and responses of patients to treatment. We discussed various biofabrication technologies, including 3D bioprinting techniques developed for characterizing tumor progression, metastasis, and response to treatment.

Graphic abstract

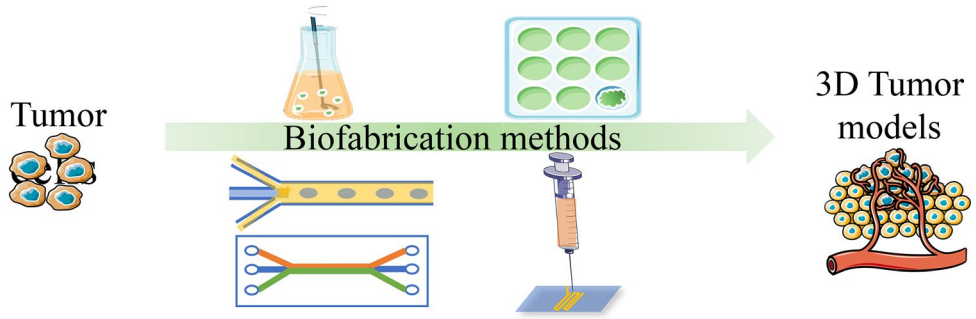

Keywords Tumor models · Biofabrication · Tumor spheroids · Microfluidic devices · 3D bioprinting

Introduction

Cancer is one of the most threatening public health problems globally [1, 2]. It is often diagnosed only at late stages, which not only delays treatment, but also impairs the oncological research on tumor development [3–5]. Animal models have been widely used in oncological research. Mice tumor models can often be prepared by radioactive or chemical activation, or genetic modification [6–8]. For instance, a liver tumor model can be developed by injecting dimethylnitrosamine (DMN) into mice to induce severe liver damage, leading to the development of liver tumors in the mice [9]. However, a prolonged induction time, a high death rate, and the randomness of phenotype and location of the induced tumors lead to low-throughput and unpredictable outcomes. Xenograft tumor implantation eases these burdens. However, these models fail to imitate the complex human tumor microenvironment and do not allow for high-throughput characterization and drug discovery under more human-like physiological conditions. In addition, real-time monitoring of tumor onset and development can be hard to achieve using animal models. With advances in tissue engineering, bioprinting, and oncology, it is possible to biofabricate a 3D

✉ Kaiming Ye
kye@binghamton.edu

[1] Department of Biomedical Engineering, Center of Biomanufacturing for Regenerative Medicine, Binghamton University, State University of New York (SUNY), PO Box 6000, Binghamton, NY 13902, USA

tumor model that can replicate tumor microenvironments in humans.

Most 3D tumor models are in the form of cancer spheroids [10–12]. Tumor and stromal cells are assembled into tumor spheroids to create clinically relevant cell–cell and cell–extracellular matrix (ECM) interactions that mimic the in vivo human tumor microenvironment [12–14]. By mimicking this microenvironment, these tumor models have emerged as an alternative to animal tumor models for oncology and drug discovery. Over the last two decades, uncontrolled tumor spheroid self-assembly techniques have evolved into more customized and controlled biofabrication technologies [15–19]. Moreover, more clinically relevant stromal cells, such as endothelial cells, immune cells, and fibroblast cells, have been successfully integrated into biofabricated tumor models, mimicking in vivo cancer cell organization and interactions [20–23]. These developments are crucial for characterizing tumor proliferation, metabolism, metastasis, and progression as well as assessing the responses of cancer cells to treatment. It has been reported that cancer cells cultured in 3D models show increased resistance to anticancer drugs and increased metastasis potential [20]. In addition, a hypoxic environment within tumor spheroids, another important and relevant characteristic of tumors, can be readily achieved by biofabrication [14]. In this review, we have focused on the various technologies developed for tumor model biofabrication.

Mechanical force and surface patterning-based tumor model development

Hanging drop

Hanging drop utilizes gravity to force cells to converge into clusters by adding a drop of a cell suspension onto the inner surface of a nonstick cell culture dish lid, as shown in Fig. 1a. Culturing the spotted cell suspension on the lid for an extended period of time, about 10–14 days, results in the formation of tumor spheroids [24]. This method has been widely used to build 3D tumor models. For instance, Yip et al. developed a hetero-spheroid liver cancer model for testing anticancer drugs using the hanging drop technique [25].

Using the same technology, Raghavan et al. generated stable and uniform ovarian cancer spheroids using a novel hanging drop plate designed for preclinical drug sensitivity analysis [29]. Following these initial studies, Eder et al. demonstrated a high-throughput hanging drop tumor model development methodology that enabled development of prostate cancer spheroids on a 96-well plate, as shown in Fig. 1b [27]. This improved hanging drop development technique; tumor model enables characterization of interactions between tumor epithelial and extracellular matrices in a high-throughput manner.

The materials used for the hanging drop technique have a profound effect on tumor spheroid development. For a long

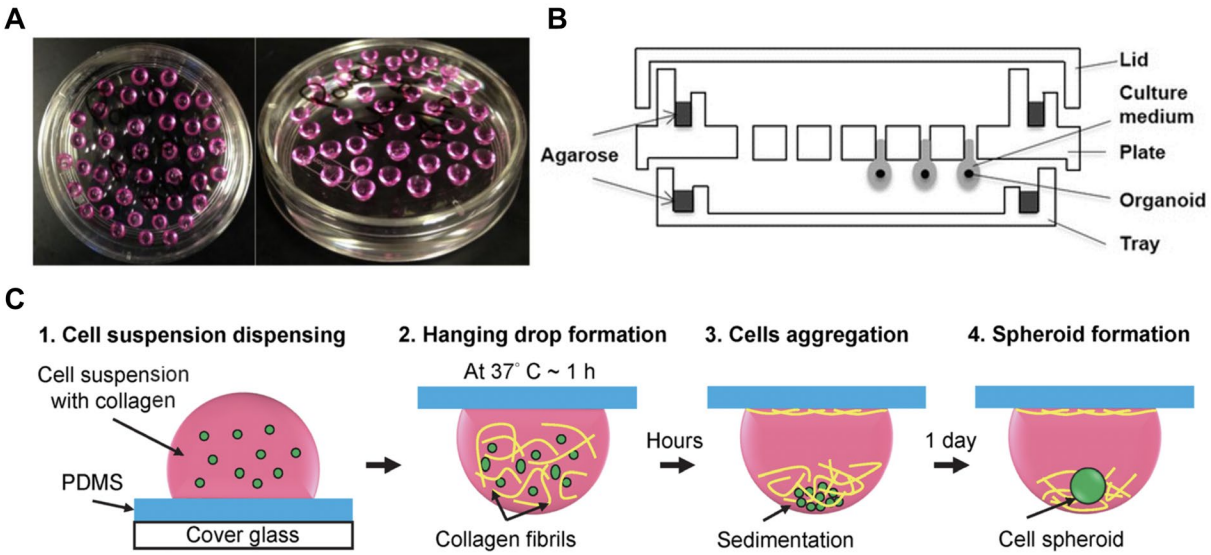

Fig. 1 Hanging drop-based tumor spheroid development. **a** The hanging drop configuration, reproduced with permission from Ref. [26]. **b** A schematic diagram of a multiwall hanging drop method for high-throughput tumor spheroid assembly, reproduced with permission from Ref. [27]. **c** Collagen fibrils are incorporated into polydimethylsiloxane-based hanging drop array (PDMS-HDA) to promote cell aggregation, reproduced with permission from Ref. [28]

time, the formation of condensed spheroids of pancreatic ductal adenocarcinoma cells (PDAC) with hanging drop methods was considered difficult because of the weak aggregation properties of these cells. To overcome this difficulty, Ware et al. assembled these spheroids by adding methylcellulose to the hanging drop solution, to serve as a thickening agent [26].

Spheroid formation can also be enhanced by incorporating several biomaterials into a hanging drop solution. For instance, Kuo et al. incorporated collagen fibrils in a polydimethylsiloxane-based hanging drop array (PDMS-HDA), which not only promoted the interaction of cell aggregates, but also expedited tumor spheroid formation (Fig. 1c) [28]. With these materials in the hanging drop, spheroids were formed within 24 h.

Tumor spheroids can be formed by hanging drop with or without an extracellular matrix. The size of tumor spheroids formed by hanging drop can be controlled by altering seeding density or the culture time. The hanging drop technique is simple and can be high-throughput. But the process is still time-consuming due to the extra time needed for drop preparation. In addition, tumor models created by hanging drop are less complex than natural tumors and they also are not perfect replicates of in vivo tumor architecture and environments.

Surface micropatterning

Another tumor model development technique is to micropattern the surface of a substrate. Micropatterned surfaces can be fabricated by soft lithography [30], which was first developed by Whitesides and colleagues [31]. This technique uses elastomeric stamps, molds, or conformable photomasks to micropattern the surface of a substrate [32]. The use of nonadherent elastomeric materials is critical to this technique. Polyethylene glycol (PEG), a biocompatible and nonadherent material, has been used to create a nonadherent surface for assembling tumor models [33]. Polydimethylsiloxane (PDMS) is another material used in micropatterning by soft lithography. Jiang et al. prepared a single-component, thermo-responsive, micropatterned poly(di(ethylene glycol)methyl ether methacrylate) (PDEGMA) film capable of releasing cell aggregates, i.e., spheroids, by lowering the temperature of the culture medium from 37 to 22 ℃, as illustrated in Fig. 2a [34].

Micropatterning provides more precise control of the size and morphology of tumor spheroids by controlling conditions for cell aggregation. This technique has been used to build a tumor model to imitate the tumor microenvironment by controlling the structure and stiffness of the matrix. For instance, Peela et al. generated a tumor model

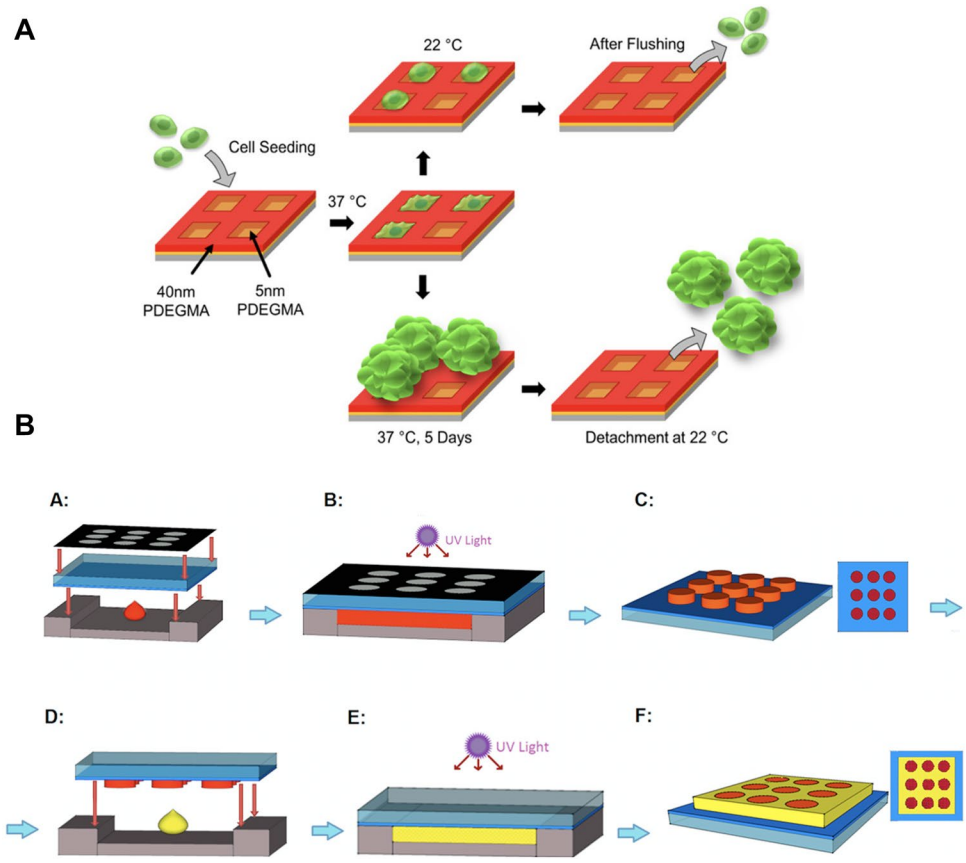

Fig. 2 Micropatterning processes for tumor model development. **a** Release of cancer spheroids from a thermo-responsive and micropatterned poly(di(ethylene glycol)methyl ether methacrylate) (PDEGMA) film, reproduced with permission from Ref. [34]. **b** A two-step micropatterning tumor model development technique for studying breast cancer cell migration, reproduced with permission from Ref. [35]

by micropatterning to study breast-cancer cell migration [35]. They developed a novel two-step photolithography technique to create a highly organized 3D tumor microenvironment that contains two distinct regions differing in stiffness (Fig. 2b). Using this model, these authors characterized the effect of tumor stiffness on breast-cancer cell migration.

Compared to the hanging drop technique, surface patterning could potentially be used to create a more sophisticated tumor microenvironment for studying how the mechanical properties of tumor matrices affect tumor behaviors and the response of tumors to treatment. However, in its current state of development, surface patterning is still less effective in creating complex and heterogenic tumor 3D structures.

Inducing tumor spheroid assembly using a nonadherent surface

Cancer cells can be forced to aggregate into spheroids by seeding them onto a nonadherent surface. A nonadherent surface can be created by coating a surface with nonadherent materials. Cells cultured on a nonadherent surface form free-floating spheroids [36, 37]. Agar and agarose were the first two biomaterials tested for generating free-floating tumor spheroids using this method. In 1971, Dalen et al. used an agar-coated plate to form L5178Y spheroids [38]. The disadvantage of using these two materials is that their coated plates can only be stored for several days. To overcome this limitation, poly(2-hydroxyethyl methacrylate) (poly-HEMA) coating has been developed for fabricating tumor spheroids using a nonadherent surface. Unlike agar or agarose, poly-HEMA-coated plates can be stored for several months. Nevertheless, poly-HEMA is expensive and the coating procedure is also time-consuming: it usually requires several hours to dissolve the polymers and overnight treatment to dry the coated plates [39].

Instead of coating techniques, ultralow (ULA) attachment substrates have been developed for manufacturing tumor spheroids using a nonadherent surface. Vinci et al. demonstrated the feasibility of growing cancer cells into tumor spheroids on a ULA 96-well plate [40]. Using a ULA plate for tumor model manufacturing is simple and high-throughput. Nevertheless, there are several limitations, including high cost and difficulty in generating complex tumor structures.

The size of cancer spheroids formed on a nonadherent surface can be controlled by varying seeding density and culture time, as demonstrated by Ma et al. [41], who showed that the size of tumor spheroids formed on a nonadherent surface is proportional both to seeding density and culture time.

Fabricating tumor spheroids by spinner culture

Spinner culture is another biofabrication technology developed for generating a large number of tumor spheroids in a more controlled fashion. This technology involves the culture of cancer cells in a spinner flask bioreactor. Continuous agitation of the culture medium in the bioreactor forces the cells to form tumor spheroids, as depicted in Fig. 3a. Using this technology, Pawlik et al. created multicellular hepatoma spheroids to ascertain amino acid uptake and metabolism in tumors [42]. This method can be combined with other techniques to construct a more complicated tumor model. For instance, Brancato et al. created human PDAC microtissues by coculturing pancreatic cancer cells (PT45) with cancer-associated fibroblasts (CAFs) within gelatin microscaffolds in a spinner flask [13]. Normal or carcinoma-associated fibroblasts were mixed with microscaffolds in a spinner flask to generate stroma-like tissues. Next, PT45 and stroma-like tissues were cocultured in the spinner flask to form a tumor-like tissue, as shown in Fig. 3a. This method can also be used to coculture tumor cells with normal tissues to interrogate their interactions. For instance, Helige et al. cocultured choriocarcinoma cells with human endometrial or decidual tissues to study trophoblast invasion [43]. A three-step spinner culture method was developed for generating this tumor model (Fig. 3b). First, rounded tissue fragments and multicellular choriocarcinoma cell spheroids were formed and transferred onto a petriPERM petri dish with a hydrophobic surface. The spheroids and tissue fragments were then transferred to a spinner flask for co-culture after connections between the tissue fragments, and choriocarcinoma spheroids were established.

Moreover, Santo et al. found that the size and morphology of tumor spheroids can be influenced by seeding density, cell type, and hydrodynamic conditions in the spinner cultures (Fig. 3c–3f) [44]. Large spheroids tend to form with a higher seeding density and lower stirring rate.

While this biofabrication technique has advantages in producing a large number of tumor spheroids, the cell damage caused by shear stress during agitation could potentially impair its application in oncological research. Moreover, size of tumor spheroids formed is hard to control with this technique.

Microfluidic-based tumor model biofabrication

Microfluidic technology offers precise control of small fluid volumes inside microscale channels. This technology has been augmented to generate tumor microcapsules by separating cancer-cell suspensions into small droplets under water/oil surface tension. The encapsulated cancer and/or stromal

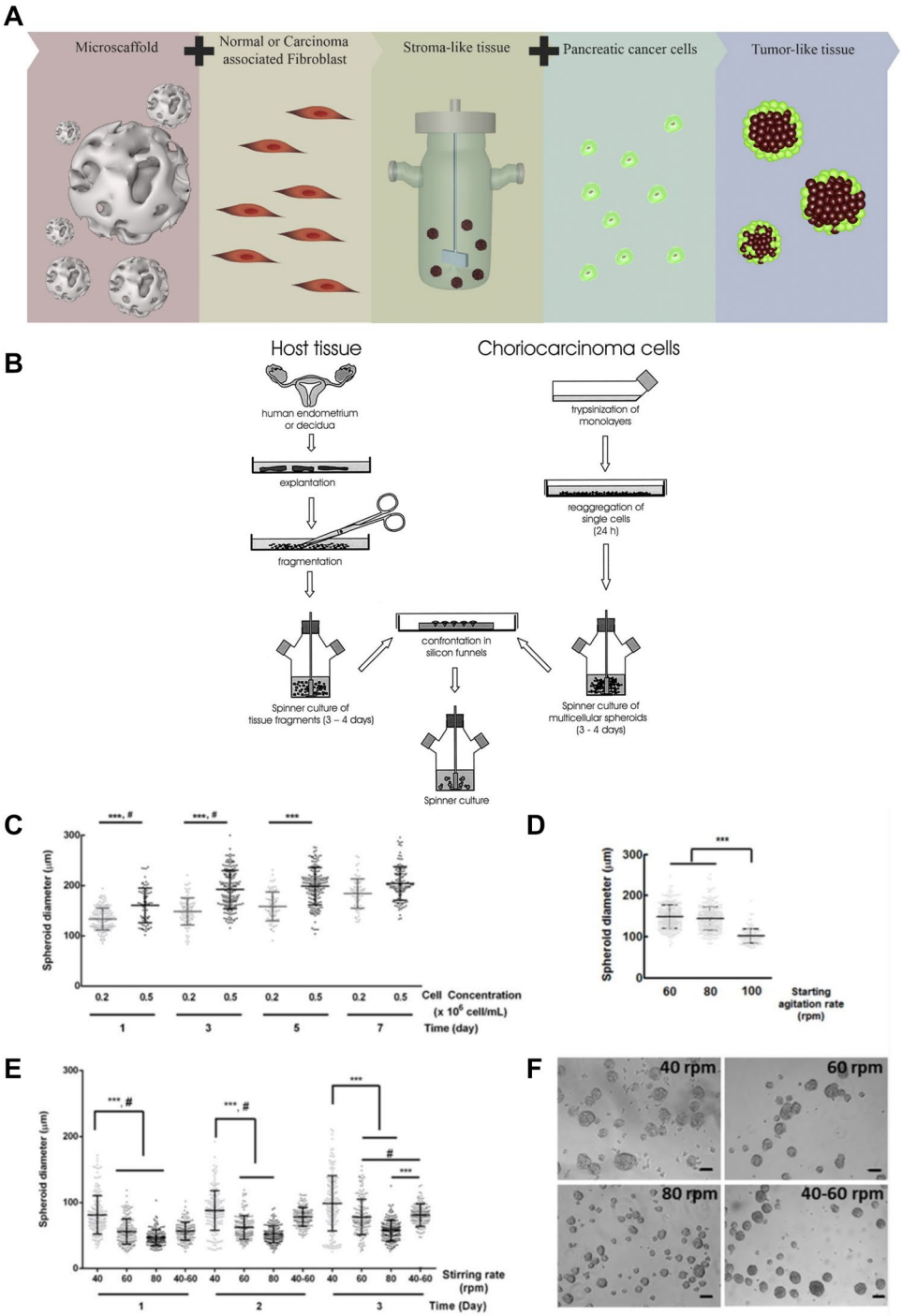

Fig. 3 Spinner cultures designed for biofabricating tumor models. **a** A spinner flask bioreactor designed for developing a pancreatic ductal adenocarcinoma cells (PDAC) model, reproduced with permission from Ref. [13]. **b** Coculture of human endometrial with decidual tissues in the spinner flask to form multicellular spheroids of choriocarcinoma cells, reproduced with permission from Ref. [43]. **c** The effect of initial cell concentration and culturing time on the diameter of MCF7 spheroids at a 60 r/min stirring rate. **d** The effect of stirring rate on the diameter of MCF7 spheroids with an inoculum of 0.2×10^6 cells/mL within 24 h. **e** The effect of stirring rate on the diameter of H460 spheroids with an inoculum of 0.2×10^6 cells/mL at day 1–3. **f** Morphology of H460 spheroids at day 3 with different stirring rate. **c**–**f**, reproduced with permission from Ref. [44]

cells develop into tumor organoids, allowing for rapid creation of larger numbers of small, uniform tumor spheroids (< 300 μm) [45, 46]. With this technology, Shintaku et al. encapsulated mouse erythroleukemia (MEL) cells inside alginate-hydrogel beads to form cancer spheroids [47]. Alginate is biocompatible and can form a hydrogel after mixing with calcium chloride, as shown in Fig. 4a. Enclosed cancer cells retain their ability to proliferate and function after gelation, as the gentle gelation does not require heat or treatment with acids or alkali. In addition, the tumor models biofabricated by this method have smaller, more uniform diameter, compared to self-assembled cancer spheroids prepared with hanging drop or nonadherent surface approaches.

Various biomaterials have been tested for microfluidic tumor model biofabrication, including gelatin, collagen, gelatin methacryloyl (GelMA) [48], and PEG-DA (poly(ethylene glycol) diacrylate) [49]. Unlike alginate, these biomaterials are derived from animal collagen,

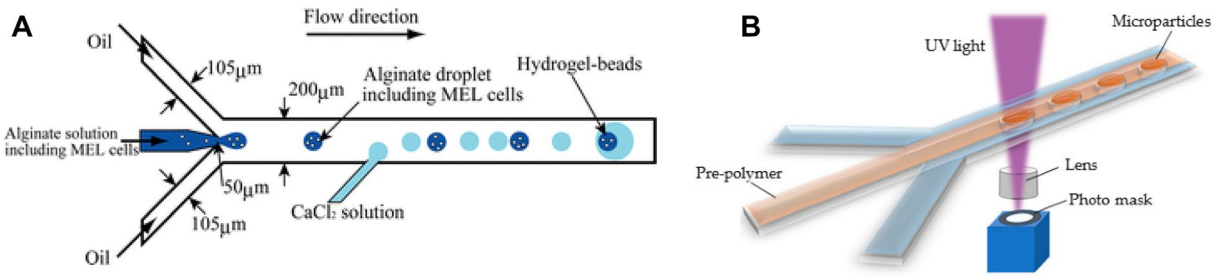

Fig. 4 Microfluidic oil–water phase processes designed for biofabricating tumor models. **a** Alginate-$CaCl_2$-based hydrogel beads production process, reproduced with permission from Ref. [47]. **b** The photo-initiator-based hydrogel beads production process, reproduced with permission from Ref. [16]

providing better cell adhesion and mechanical properties [49]. Crosslinking of these biomaterials into hydrogel beads can be achieved by adding a photo-initiator such as 2-hydroxy-1-(4-(2-hydroxyethoxy)phenyl)-2-methyl-1-propanone (Irgacure 2959) [50, 51] or lithium acylphosphinate salt (LAP) to the solution [52]. Photo-initiators can be activated by UV (about 265 nm wavelength) irradiation that catalyzes the cross-linking rapidly, in approximately 30 min for Irgacure 2959 and 30 s for LAP.

Collagen-based hydrogels are digestible by proteases, facilitating reorganization of the cell microenvironment through extracellular matrix secreted from cells [51]. In addition, microfluidic devices can be employed to produce more complicated tumor organoid structures, such as multilayer capsules. In a recent study, Alessandri et al. designed a multichannel coaxial extruder that allows different materials to flow in parallel after extrusion, as shown in Fig. 5a and 5b [53]. Materials in the coaxial tips, going from the innermost to outermost regions, are: cell suspension, extracellular matrix, and alginate hydrogel, respectively.

Spontaneous instability of multilayer materials leads to merger of the outside materials to form shells covering the inner contents. This method can be applied to generate submillimetric spheres with a soft cell-containing extracellular matrix core and a rigid alginate shell that surrounds the core to protect the structure of the beads. This technique resolves the dilemma that cells need soft hydrogels to survive, while the scaffolds need high mechanical strength to maintain their structure.

The multilayer extrusion technique has numerous applications to tumor model biofabrication, as cancer cells always interact with different stromal cells in a high order of spatial complexity. For instance, PDACs are always surrounded by cancer-associated fibroblasts, macrophages, regulatory T cells, and other stromal cells [21]. The multilayer capsules in which PDACs are enveloped by these cells will accurately replicate the in vivo pancreatic tumor microenvironment.

This biofabrication technology enables the combination of two distinct biomaterials to form a more sophisticated

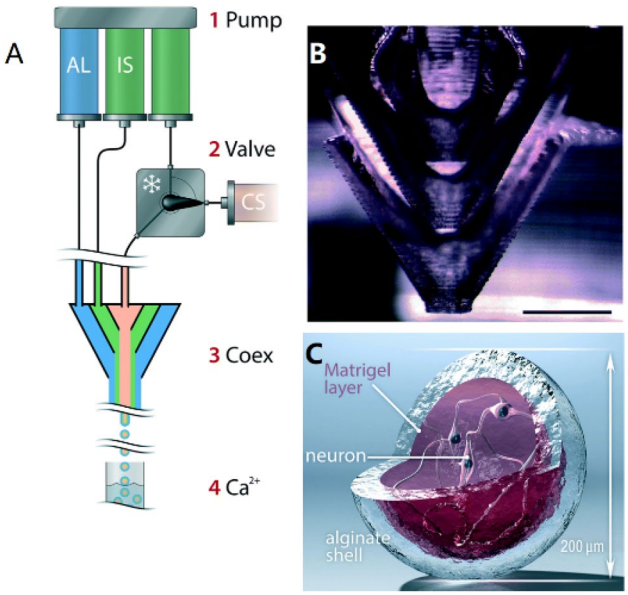

Fig. 5 Production of multilayer hydrogel-beads via coaxial extrusion. **a** Instrument setup. **b** Optical image of side view of multichannel extruder tips. **c** Schematic diagram showing the components assembled in the hydrogel-beads, reproduced with permission from Ref. [53]

cancer-organoid structure, enabling a post-gelation control. For instance, plasmonic gold nanorods can be integrated into shell materials to form thermal trigger-releasing capsules [22]. In this fashion, poly(lactic-co-glycolic) acid-containing plasmonic gold nanorod-encapsulated growth factors can be incorporated into a gelatin methacrylate core. Laser irradiation of the capsules heats the plasmonic gold nanorods and breaks the shell materials to release growth factors into surrounding areas from the core. This technique permits temporospatial control of the gradient of growth factors in the tumor models. It is, therefore, ideal for studying cancer cell migration.

Microfluidic techniques can also be utilized for biofabricating a tumor-on-a-chip. Tumor-on-a-chip is a

microfluidic device that can precisely control the flow of small volumes of cell culture medium continuously through microchannels that connect tumor spheroids or organoids with their interacting tissues or organs such as lymph nodes [54–57]. For most cancer cells, cellular physiological events such as immune responses, cell invasion, and cell migration are highly dependent upon a vascular system. Thus, a tumor-on-a-chip enables investigations of crosstalk between tumors and their supporting or targeting tissues or organs. For instance, Shim et al. assembled an ex vivo tumor-on-a-chip consisting of tumor tissues and lymph nodes, as shown in Fig. 6a and 6b. [58]. Using this chip, they characterized lymph node tissue-induced immunosuppression in tumors. In another study, Chen et al. designed a system that forms self-organized human microvascular networks within 4–5 days, following the perfusion of a tumor cell suspension into an extravasation [57]. Human umbilical vein endothelial cells (HUVECs) seeded onto the chip elongated and formed vacuoles, inducing the self-assembly of microvascular networks that allow tumor cells to pass through them under perfusion (Fig. 6c and 6d). With this technique, the researchers tracked the extravasation of tumor cells on a single-cell

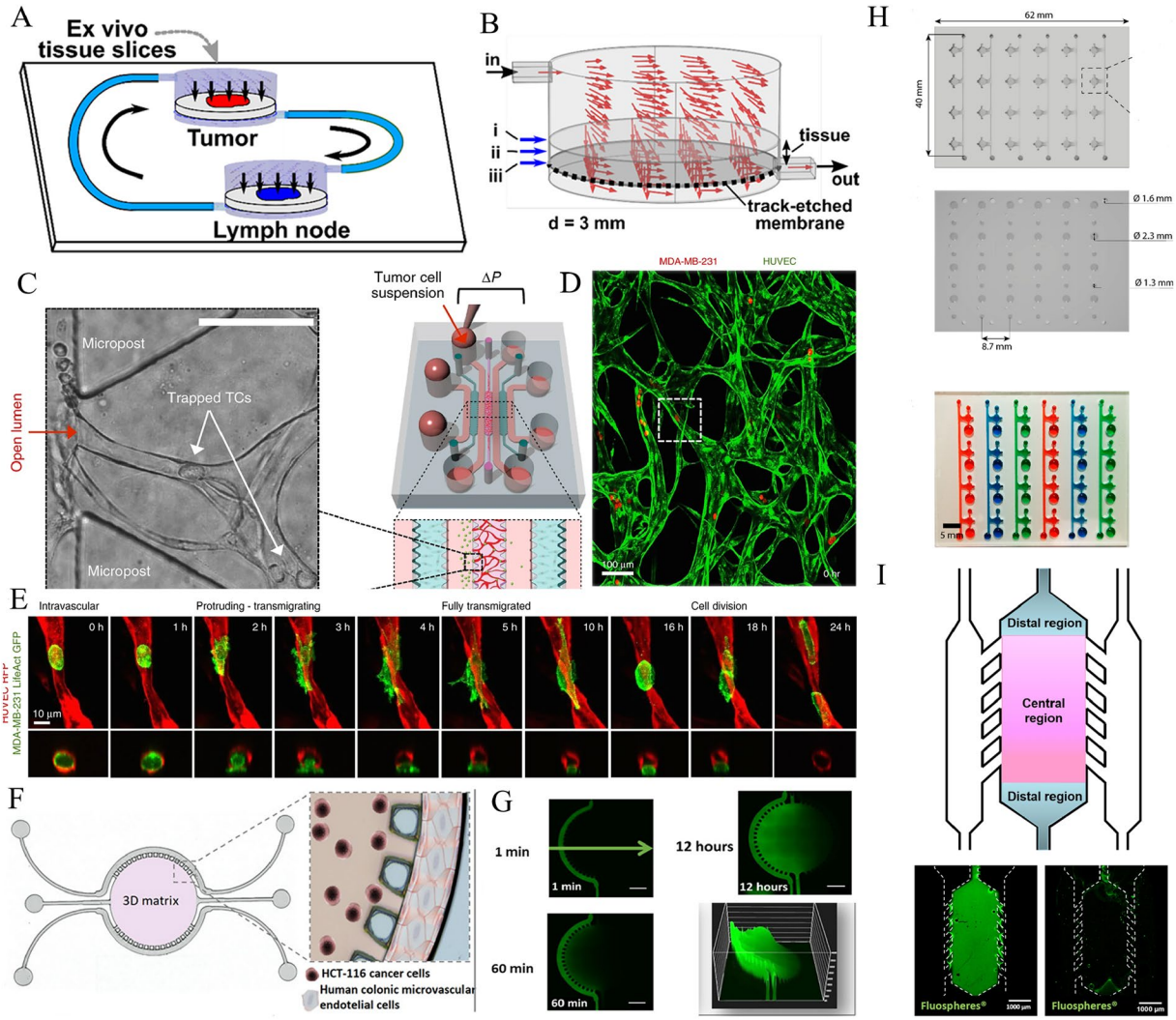

Fig. 6 Microfluidic-based tumor-on-a-chip biofabrication**. a**, **b** A schematic diagram of tumor tissues and lymph nodes co-culture systems, reproduced with permission from Ref. [58]. **c**, **d** Tumor-on-a-chip with perusable self-assembly vascular systems, reproduced with permission from Ref. [57]. **e** Micrographs of tumor cell extravasation from the microvasculature and subsequently undergoing cell division over 24 h, reproduced with permission from Ref. [57]. **f** A schematic diagram of a microfluidic system that separates tumor cells and culture medium with a layer of endothelial cells, reproduced with permission from Ref. [54]. **g** Fluorescent micrographs of diffusion that forms a gradient of drug reagents inside the chip, reproduced with permission from Ref. [54]. **h** Optical images of microfluidic arrays with multiple chambers in one line and multiple lines in one chip, reproduced with permission from Ref. [59]. **i** A schematic diagram to indicate the microfluidic-based enzymatic method for cell recovery, reproduced with permission from Ref. [60]

level and determined the kinetics by high-resolution imaging (Fig. 6e).

This technique can also be used for drug discovery. Carvalho et al. characterized the effect of gemcitabine on colorectal tumor cells using a tumor-on-a-chip system [54]. This system produces well-controlled gradients of drugs in the fluid and allows the diffusion through human colonic microvascular endothelial cells (Fig. 6f and 6g). Efforts have also been made to improve throughput and cell recovery of the microfluid chips [59, 60]. Using PDMS-based soft lithography, a microfluidic array capable of testing multiple doses in quadruplet of target compounds has been fabricated, as illustrated in Fig. 6h. Through a collagenase-based enzymatic method and microfluidic device, the cells seeded onto a 3D scaffold can be readily harvested with less damage for additional assays such as qPCR or flow cytometry (Fig. 6i). All these designs are critical for increasing the throughput of cancer model chips.

While the microfluidic biofabrication technique allows a precise control of small volume fluids to generate hydrogel beads with a multiple layer structure, the spatial complexity of tumor models built with this technique still remains limited. Tumor-on-a-chip is a considerable advance in tumor modeling. The standardization of tumor-on-a-chip design and fabrication remains challenging: data acquired from these tests are usually hard to compare among different laboratories. Maintenance of microtissues during extended cultures on the chip is another challenge. In addition, the development of a cell-culture medium that can meet nutrient needs for all microtissues grown on the chip is still a difficult task. To address these challenges, tumor-on-a-chip represents a revolutionary tumor-modeling technique amenable to simulating interorgan crosstalk between tumors and their surrounding or targeting tissues and organs. This ability is of paramount importance for drug discovery and oncological research.

Bioprinting

3D bioprinting is one of the bioadditive manufacturing technologies that have been developed for biofabricating tissue constructs. With programmed robotic control, 3D bioprinting offers accurate deposition of cells and biomaterials in a layer-by-layer fashion to build a complex 3D tissue structure, enabling the design and manufacturing of tumor organoids similar to in vivo tumors [61–63]. Various bioprinting modalities, including stereolithography, inkjet bioprinting, laser-assisted bioprinting, extrusion-based bioprinting, and electrospinning-based bioprinting, have been developed and applied to tumor model biofabrication, as summarized in Table 1.

Applying bioprinting to biofabricate tumor models provides unprecedented advantages. Many natural biomaterials, such as decellularized extracellular matrices, can be used for creating biomimetic and extracellular matrix-like niches with desired mechanical and morphological characteristics for growth of tumor cells [62, 63, 78]. Furthermore, multiple types of cells and tissues can be assembled into cancer organoids to form a complex tumor structure within a scaffold [78, 79].

Tumor-model bioprinting involves several elements, including bioink, cross-linking, and deposition. Bioink can be formed with or without cells. A biomaterial used for constituting a bioink should have excellent shear thinning rheological properties for fluidic deposition, adequate gelation or cross-linking properties for tissue patterning, and biocompatibility to keep cells alive and functioning during and after printing. Both natural and synthetic biomaterials, including decellularized extracellular matrix, fibrin, hyaluronic acid, collagen, elastin, Matrigel, gelatin, chitosan, alginate, pullulan, poly(lactic acid) (PLA), poly(glycolic acid) (PGA), poly(lactic acid-co-glycolic acid) (PLGA), poly(ethylene glycol) (PEG), and poly(caprolactone) (PCL), have been examined for composing bioinks for 3D tumor printing. Bioinks without cells are used to print acellular scaffolds. For acellular scaffolds, cells can be seeded into the scaffolds after printing [80]. Viscosity, modulus of elasticity, yield strength, reactivity, and degradation of bioinks are critical to generating a desired tumor model [79, 81].

Acellular tumor model bioprinting

Cells are usually vulnerable to stresses such as shear stress, high temperature, or high pressure applied during bioprinting. High temperature or pressure might, however, be necessary for constructing more complicated structures such as a lumen structure orvasculature network within printed tumor organoids. Moreover, the use of toxic solvents or cross-linking reagents might be required for printing high-resolution scaffolds [79, 82, 83]. In these cases, the printing of acellular scaffolds is preferred. Cells can be seeded into the scaffolds after printing.

Zhu et al. printed a biomimetic bone structure for investigating metastasis and invasion of breast cancers into bone tissues (Fig. 7a) [84]. These investigators studied the metastasis of MDA-MB-231 and MCF-7 breast cancer cells in bone matrices printed using a bioink consisting of hydroxyapatite nanoparticles suspended in PEG-diacrylate (PEGDA) hydrogel, as shown in Fig. 7b. Cells were seeded onto the matrices after printing due to a long cross-linking process to form a scaffold after printing.

While printing an acellular scaffold enables the use of widely available biomaterials for creating a desired anatomical tumor structure, seeding cells onto the scaffold

Table 1 Various bioprinting technologies developed for tumor model biofabrication

Printing modality	Tumor model	Advantage	Disadvantage	Reference
Inkjet bioprinting	Precise patterning of multiple cell types into a tumor model	-Simple -Low cost -Droplet extrusion -High cell viability	-Discontinuous printing -Low cell density	[64–66]
Laser-assisted bioprinting	Precise control of spatial patterning of tumor organoids	-Suitable for bioink with a wide range of viscosities -High cell viability -Able to print multiple layers in one droplet	-High cost -Complex -Low cell density	[67–69]
Extrusion-based bioprinting	Precise layer by layer printing of multiple materials along with multiple cells including cancer cells and their surrounding cells	-High cell density -Continuous printing with a high viscosity bioink. -Enables multi-material printing and complex spatial structure	-Low resolution -Low cell viability	[70–72]
Stereolithography	High fidelity of tumor structures that represent the complex tumor micro-environment including purfusable vasculatures, nerve conduits, etc	-High resolution -High cell viability	-Sophisticated -Limited choice of cross-linkers and bioinks -Waste of cells and materials after printing	[17, 64] [73–75]
Electrospinning-based bioprinting	Incorporating micro/nanostructured biomaterials into printed tumor models	-High resolution -Complex 3D tumor structure	-Complex -High cost -Impossible to use a cell-laden bioink during printing	[17, 64] [76, 77]

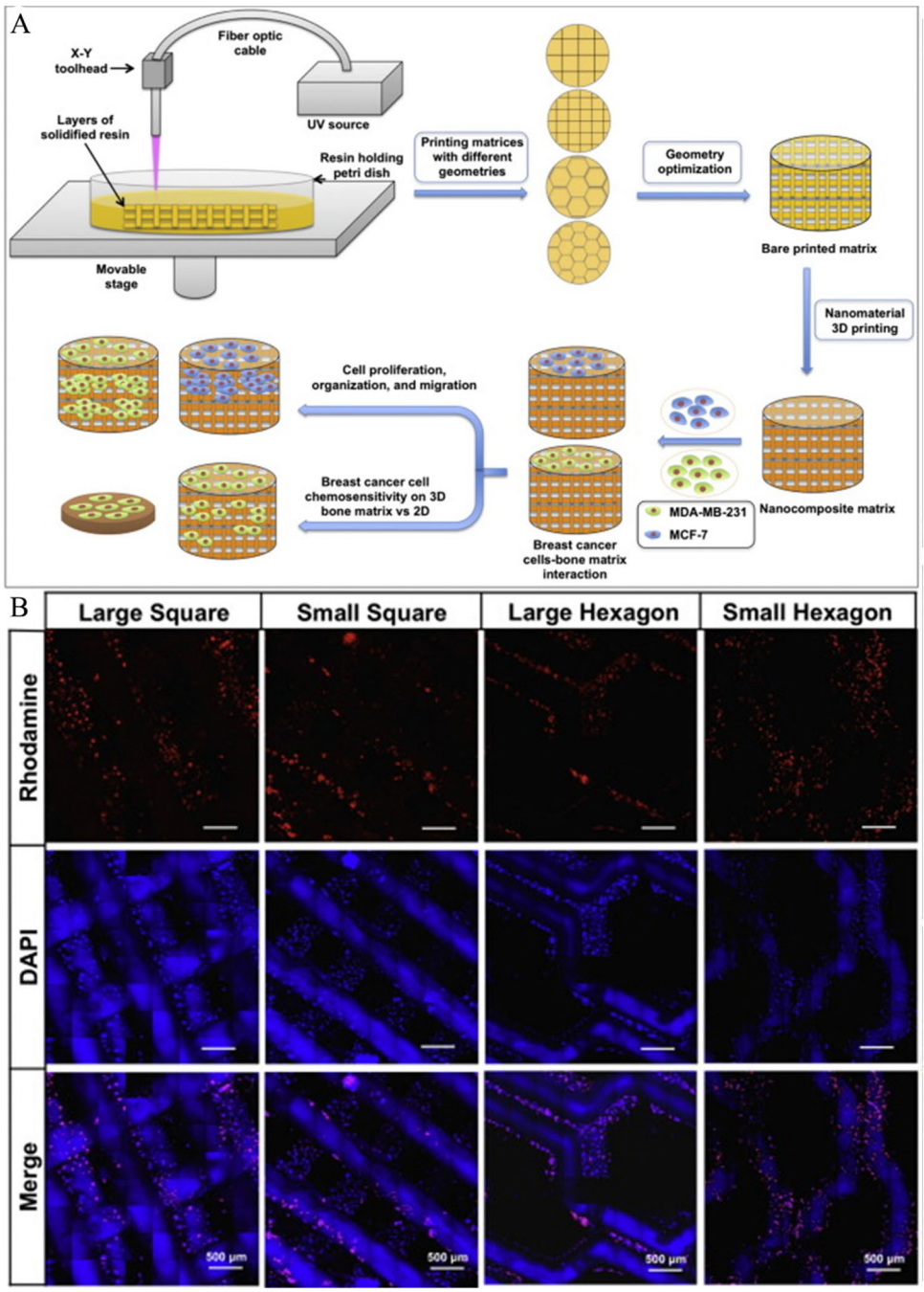

Fig. 7 Bioprinted metastasis tumor models. **a** 3D bioprinting of a metastasis breast cancer model, reproduced with permission from Ref. [84]. **b** Confocal images of MDA-MB-231 cells on 3D-bioprinted bone matrices, stained for phalloidin (red) and nuclei (blue), reproduced with permission from Ref. [84]

after printing is a challenge. Cells seeded onto the surface of a scaffold usually experience a more 2D-like microenvironment. Another challenge is the biological activity of the biomaterials used for printing. Many biomaterials have excellent shear-thinning properties but poor biological activity. They are inert to cells and cells attach poorly to these biomaterials. To improve cell attachment, adhesion molecules can be coated on the surface of these biomaterials. For instance, polydopamine (PDA) can be coated onto the surface of poly (lactic acid) (PLA) scaffolds to promote type I collagen immobilization on the scaffold, thereby increasing osteoinductivity of 3D printed PLA scaffolds [81]. RGD peptide conjugation can also improve cell attachment on the printed scaffolds [85, 86].

Tumor model bioprinting

A sophisticated tumor model can be bioprinted using a bioink encompassing both cancer and stromal cells. These printed tumor models replicate the complexity of tumor anatomical structures by re-establishing physiological cell communication, including cell–cell and cell–extracellular

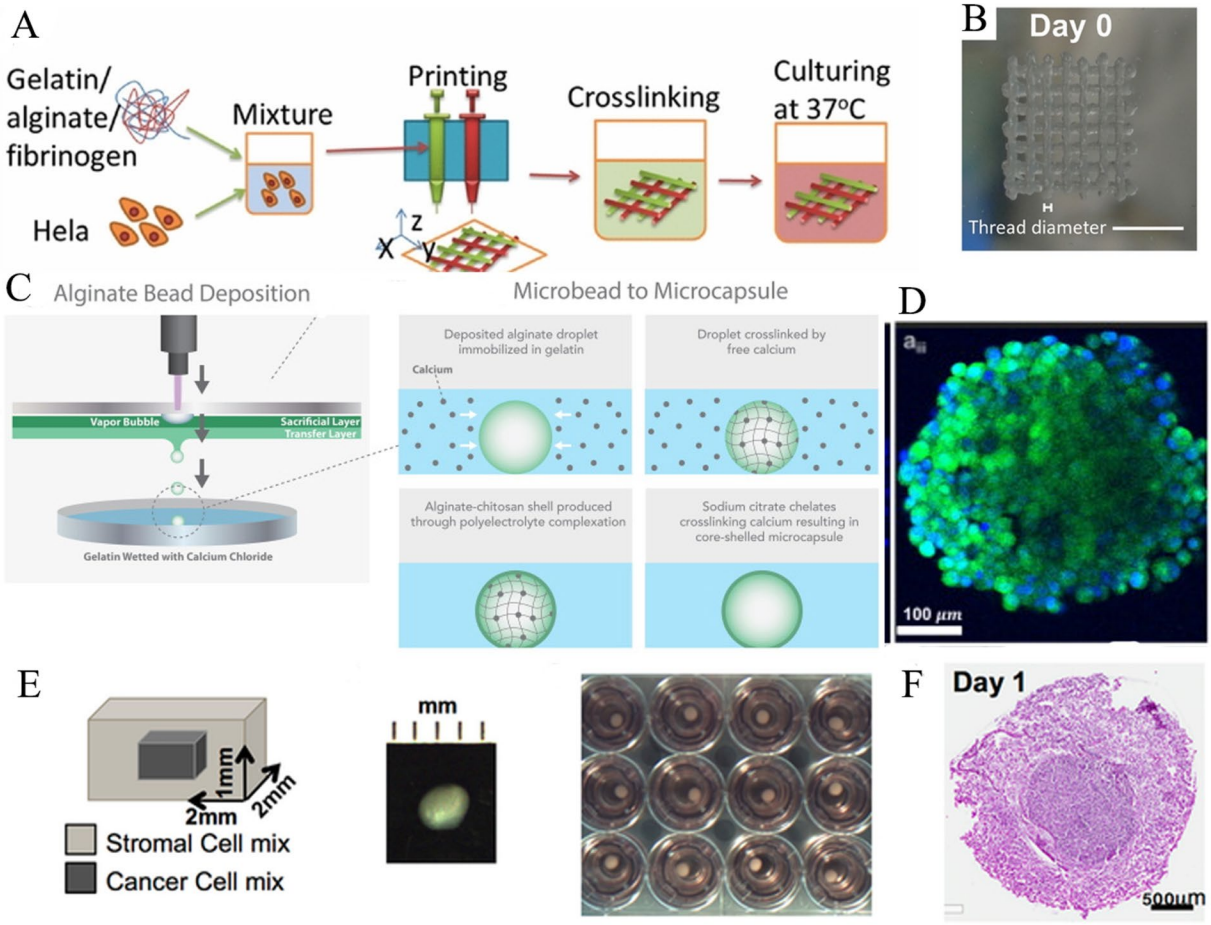

Fig. 8 A 3D bioprinted tumor model. **a**, **b** A schematic diagram of the 3D HeLa cells/hydrogel printing process, and an optical image of the scaffold after printing, reproduced with permission from Ref. [70]. **c**, **d** Laser-assisted 3D bioprinting, and fluorescent micrographs of spheroids, reproduced with permission from Ref. [67]. **e**, **f** A schematic diagram of a central cancer pocket surrounded by a stromal cell matrix, and H&E-stained 3D tumor tissue formed one day after printing, reproduced with permission from Ref. [87]

matrix interactions [22]. For instance, a bioink containing 10% gelatin, 1% sodium alginate, 2% fibrinogen, and HeLa cells can be used to construct cancer organoids by layer-by-layer printing (Fig. 8a and 8b) [70]. Cancer cells printed within these hydrogels showed a higher proliferation rate and high matrix-metalloproteinase protein expression. Laser-assisted bioprinting generates bioink droplets through focused lasers with precise location and size control [67–69]. The Corr group designed a laser-assisted 3D bioprinting technique to generate core–shell microcapsules (Fig. 8c and 8d) [67]; they were able to generate microcapsules with controlled size by controlling beam size and laser energy. While the laser-printing technique enables the printing of a core-shelled structure, it is less effective in printing multiple biomaterials in order to create a heterogenic tumor microenvironment.

Bioprinting enables the creation of multicellular tumor constructs with the desired tumor heterogeneity and anatomy by depositing cancer cells along with interacting stromal cells such as endothelial cells and immune cells in a more controlled and orderly fashion. The creation of these complicated anatomical tumor structures improves the overall biological relevance of tumor models. Langer et al. used a continuous deposition technology coupled with multiple deposition heads to print stromal and cancer cells into a complex tumor tissue structure similar to an in vivo tumor structure (Fig. 8e) [87]. In this model, the biomaterial containing cancer cells was in the center surrounded by stromal cells with desired positions and ratios. Unlike hydrogels made through coaxial nozzle-based microfluidic processes, this process enables establishment of tumor models with higher volume to include more cells in the model, and a multicore structure to mimic human tumor tissues in vivo [88].

In order to achieve the desired physicochemical and/or mechanical properties, a mixture of different biomaterials can be incorporated into a bioink. For instance, hyaluronic acid can be blended with type I collagen to improve the printability of the collagen by elevating its viscosity and

gelation ability [89]. GelMA can be mixed with PEGDA to create tumor angiogenesis models with microvasculature in a pattern [90]. On the other hand, some biocompatible materials can be temporally added to a bioink to increase the printability of the bioink. For example, Freeman et al. blended heat-treated gelatin with fibrinogen and turned unprintable fibrinogen into a printable biomaterial [91]. These improvements in the mixture of biomaterials expand the choice of bioinks and enhance the resolution of 3D bioprinting.

Nevertheless, 3D bioprinting is still limited by printing resolution determined by physical and mechanical conditions. The resolution of extrusion-based 3D bioprinting is limited by the diameter of the nozzle, which can vary from a few micrometers to millimeters [92]. Cell-laden bioinks are also fragile, and vulnerable to temperature and shear stress. The blended cells will affect the printability of the bioinks [91]. Thus, formulation of adequate varieties of bioinks for tumor model printing is critical. The low throughput of 3D bioprinting is another challenge to its ability to create more heterogeneous tumor structures.

Challenges in tumor model biofabrication

The biofabrication of tumor models has advanced the field of oncology and has led to the discovery of numerous anticancer drugs. These tumor models possess improved complexity and heterogeneity that replicate in vivo tumor structure and the tumor microenvironment. It is expected that these models can be used to replace animal models for drug screening and validation. While 3D bioprinting offers a better solution for creating more complicated anatomical structures needed in tumor models, incorporation of perfusable vasculature and/or immune networks into the tumor models by bioprinting remains a challenge. The incorporation of nervous systems or creation of innervated tumor models is another challenge. More printable bioinks need to be formulated in order to construct these tumor structures. Increased throughput of 3D bioprinting will eventually make 3D printing technology available for high-throughput tumor model biofabrication.

While microfluidic biofabrication can be high-throughput, the complexity of tumor models built using this technology is limited. Use of coaxial microfluidic channels can potentially allow for creation of multilayer hydrogel-beads that increase the complexity of the tumor models. In general, heterogeneity of these tumor models is relatively low, as compared to 3D-bioprinted tumor models. As the ability to fabricate high-throughput tumor models is pivotal to drug discovery, a combination of several biofabrication techniques might be needed to achieve its high-throughput-potential. More studies are needed to meet this requirement.

3D tumor models can be used for personalized cancer medicine. Personalized tumor models replicating the same characteristics as the original tumor of the patient is highly desired. First, personalized tumor models are considered more accurate predictors of the efficacy of different treatment methods. These models also have great potential in gene–drug correlation studies and preclinical screening of anticancer drugs. For instance, Parlato et al. generated a microfluidic 3D model for determining the effectiveness of immunotherapy by tracking the behavior of human dendritic cells toward tumor cells [93]. Combining this microfluidic 3D model with patient-derived tumor organoids could offer better predictive capability of immunotherapy protocols. It is thus hoped that greater numbers and types of human tumor-like tumor models can be created by integrating several tissue biofabrication techniques.

Author contributions ML and XS were involved in conceptualization, writing the original draft; KY and SJ helped in writing, review and editing; and KY contributed to the supervision.

Declarations

Conflict of interest The authors declare that there is no conflict of interest.

Ethical approval This article does not contain any studies with human or animal subjects performed by any of the authors.

References

1. Fukui M, Suzuki K, Matsunaga T et al (2019) Importance of smoking cessation on surgical outcome in primary lung cancer. Ann Thorac Surg 107(4):1005–1009. https://doi.org/10.1016/j.athoracsur.2018.12.002
2. Siegel RL, Miller KD (2020) Jemal A (2020) Cancer statistics. Ca-Cancer J Clin 70(1):7–30. https://doi.org/10.3322/caac.21590
3. Kerr A, Ross E, Jacques G et al (2018) The sociology of cancer: a decade of research. Sociol Health Illn 40(3):552–576. https://doi.org/10.1111/1467-9566.12662
4. Rossi SH, Prezzi D, Kelly-Morland C et al (2018) Imaging for the diagnosis and response assessment of renal tumours. World J Urol 36(12):1927–1942. https://doi.org/10.1007/s00345-018-2342-3
5. Baker LA, Tiriac H, Clevers H et al (2016) Modeling pancreatic cancer with organoids. Trends Cancer 2(4):176–190. https://doi.org/10.1016/j.trecan.2016.03.004
6. Buss LA, Mandani A, Phillips E et al (2018) Characterisation of a mouse model of breast cancer with metabolic syndrome. Vivo 32(5):1071–1080
7. Bimonte S, Barbieri A, Cascella M et al (2019) Naloxone counteracts the promoting tumor growth effects induced by morphine in an animal model of triple negative breast cancer. Vivo 33(3):821–825
8. Li L, Liang Y, Kang L et al (2018) Transcriptional regulation of the Warburg effect in cancer by SIX1. Cancer Cell 33(3):368–385. https://doi.org/10.1016/j.ccell.2018.01.010

9. Tolba R, Kraus T, Liedtke C et al (2015) Diethylnitrosamine (DEN)-induced carcinogenic liver injury in mice. Lab Anim 49(1 Suppl):59–69. https://doi.org/10.1177/0023677215570086
10. Asghar W, El Assal R, Shafiee H et al (2015) Engineering cancer microenvironments for in vitro 3-D tumor models. Mater Today (Kidlington) 18(10):539–553. https://doi.org/10.1016/j.mattod.2015.05.002
11. McLane JS, Ligon LA (2016) Stiffened extracellular matrix and signaling from stromal fibroblasts via osteoprotegerin regulate tumor cell invasion in a 3-D tumor in situ model. Cancer Microenviron 9(2–3):127–139. https://doi.org/10.1007/s12307-016-0188-z
12. Weiswald LB, Bellet D, Dangles-Marie V (2015) Spherical cancer models in tumor biology. Neoplasia 17(1):1–15. https://doi.org/10.1016/j.neo.2014.12.004
13. Brancato V, Comunanza V, Imparato G et al (2017) Bioengineered tumoral microtissues recapitulate desmoplastic reaction of pancreatic cancer. Acta Biomater 49:152–166. https://doi.org/10.1016/j.actbio.2016.11.072
14. DelNero P, Lane M, Verbridge SS et al (2015) 3D culture broadly regulates tumor cell hypoxia response and angiogenesis via pro-inflammatory pathways. Biomaterials 55:110–118. https://doi.org/10.1016/j.biomaterials.2015.03.035
15. Colosi C, Shin SR, Manoharan V et al (2016) Microfluidic bioprinting of heterogeneous 3D tissue constructs using low-viscosity bioink. Adv Mater 28(4):677–684. https://doi.org/10.1002/adma.201503310
16. Wang XH, Liu JF, Wang PZ et al (2018) Synthesis of biomaterials utilizing microfluidic technology. Genes-Basel 9(6):283. https://doi.org/10.3390/genes9060283
17. Heinrich MA, Liu W, Jimenez A et al (2019) 3D Bioprinting: from benches to translational applications. Small 15(23):e1805510. https://doi.org/10.1002/smll.201805510
18. Kacarevic ZP, Rider PM, Alkildani S et al (2018) An introduction to 3D bioprinting: possibilities, challenges and future aspects. Materials (Basel) 11(11):2199. https://doi.org/10.3390/ma11112199
19. Ji S, Guvendiren M (2017) Recent advances in bioink design for 3D bioprinting of tissues and organs. Front Bioeng Biotechnol 5:23. https://doi.org/10.3389/fbioe.2017.00023
20. Riedl A, Schlederer M, Pudelko K et al (2017) Comparison of cancer cells in 2D vs 3D culture reveals differences in AKT-mTOR-S6K signaling and drug responses. J Cell Sci 130(1):203–218. https://doi.org/10.1242/jcs.188102
21. Francescone R, Vendramini-Costa DB, Franco-Barraza J, et al (2018) NetrinG1/NGL-1 Axis promotes pancreatic tumorigenesis through cancer associated fibroblast derived nutritional supply and immunosuppression. bioRxiv 330209 https://doi.org/10.1101/330209
22. Meng F, Meyer CM, Joung D et al (2019) 3D bioprinted in vitro metastatic models via reconstruction of tumor microenvironments. Adv Mater 31(10):e1806899. https://doi.org/10.1002/adma.201806899
23. Wang S, Ghezzi CE, Gomes R et al (2017) In vitro 3D corneal tissue model with epithelium, stroma, and innervation. Biomaterials 112:1–9. https://doi.org/10.1016/j.biomaterials.2016.09.030
24. Vorsmann H, Groeber F, Walles H et al (2013) Development of a human three-dimensional organotypic skin-melanoma spheroid model for in vitro drug testing. Cell Death Dis 4:e719. https://doi.org/10.1038/cddis.2013.249
25. Yip D, Cho CH (2013) A multicellular 3D heterospheroid model of liver tumor and stromal cells in collagen gel for anti-cancer drug testing. Biochem Biophys Res Commun 433(3):327–332. https://doi.org/10.1016/j.bbrc.2013.03.008
26. Ware MJ, Colbert K, Keshishian V et al (2016) Generation of homogenous three-dimensional pancreatic cancer cell spheroids using an improved hanging drop technique. Tissue Eng Part C Methods 22(4):312–321. https://doi.org/10.1089/ten.tec.2015.0280
27. Eder T, Eder IE (2017) 3D hanging drop culture to establish prostate cancer organoids. Methods Mol Biol 1612:167–175. https://doi.org/10.1007/978-1-4939-7021-6_12
28. Kuo CT, Wang JY, Lin YF et al (2017) Three-dimensional spheroid culture targeting versatile tissue bioassays using a PDMS-based hanging drop array. Sci Rep 7(1):4363. https://doi.org/10.1038/s41598-017-04718-1
29. Raghavan S, Ward MR, Rowley KR et al (2015) Formation of stable small cell number three-dimensional ovarian cancer spheroids using hanging drop arrays for preclinical drug sensitivity assays. Gynecol Oncol 138(1):181–189. https://doi.org/10.1016/j.ygyno.2015.04.014
30. Wang W, Itaka K, Ohba S et al (2009) 3D spheroid culture system on micropatterned substrates for improved differentiation efficiency of multipotent mesenchymal stem cells. Biomaterials 30(14):2705–2715. https://doi.org/10.1016/j.biomaterials.2009.01.030
31. Xia Y, Whitesides GM (1998) Soft lithography. Ann Rev Mater Sci 28(1):153–184. https://doi.org/10.1146/annurev.matsci.28.1.153
32. Rogers JA, Nuzzo RG (2005) Recent progress in soft lithography. Mater Today 8(2):50–56. https://doi.org/10.1016/s1369-7021(05)00702-9
33. Zhang M, Desai T, Ferrari M (1998) Proteins and cells on PEG immobilized silicon surfaces. Biomaterials 19(10):953–960. https://doi.org/10.1016/s0142-9612(98)00026-x
34. Jiang S, Lyu B, Muller M et al (2018) Thickness-encoded micropatterns in one-component thermoresponsive polymer brushes for culture and triggered release of pancreatic tumor cell monolayers and spheroids. Langmuir 34(48):14670–14677. https://doi.org/10.1021/acs.langmuir.8b03040
35. Peela N, Sam FS, Christenson W et al (2016) A three dimensional micropatterned tumor model for breast cancer cell migration studies. Biomaterials 81:72–83. https://doi.org/10.1016/j.biomaterials.2015.11.039
36. Lin RZ, Chou LF, Chien CC et al (2006) Dynamic analysis of hepatoma spheroid formation: roles of E-cadherin and beta1-integrin. Cell Tissue Res 324(3):411–422. https://doi.org/10.1007/s00441-005-0148-2
37. Su G, Zhao Y, Wei J et al (2013) The effect of forced growth of cells into 3D spheres using low attachment surfaces on the acquisition of stemness properties. Biomaterials 34(13):3215–3222. https://doi.org/10.1016/j.biomaterials.2013.01.044
38. Dalen H, Burki HJ (1971) Some observations on the three-dimensional growth of L5178Y cell colonies in soft agar culture. Exp Cell Res 65(2):433–438. https://doi.org/10.1016/0014-4827(71)90023-1
39. Kuroda Y, Wakao S, Kitada M et al (2013) Isolation, culture and evaluation of multilineage-differentiating stress-enduring (Muse) cells. Nat Protoc 8(7):1391–1415. https://doi.org/10.1038/nprot.2013.076
40. Vinci M, Gowan S, Boxall F et al (2012) Advances in establishment and analysis of three-dimensional tumor spheroid-based functional assays for target validation and drug evaluation. BMC Biol 10:29. https://doi.org/10.1186/1741-7007-10-29
41. Ma HL, Jiang Q, Han S et al (2012) Multicellular tumor spheroids as an in vivo-like tumor model for three-dimensional imaging of chemotherapeutic and nano material cellular penetration. Mol Imag 11(6):487–498. https://doi.org/10.2310/7290.2012.00012
42. Pawlik TM, Souba WW, Sweeney TJ et al (2000) Amino acid uptake and regulation in multicellular hepatoma spheroids. J Surg Res 91(1):15–25. https://doi.org/10.1006/jsre.2000.5888

43. Helige C, Hagendorfer G, Smolle J et al (2001) Uterine natural killer cells in a three-dimensional tissue culture model to study trophoblast invasion. Lab Invest 81(8):1153–1162. https://doi.org/10.1038/labinvest.3780327
44. Santo VE, Estrada MF, Rebelo SP et al (2016) Adaptable stirred-tank culture strategies for large scale production of multicellular spheroid-based tumor cell models. J Biotechnol 221:118–129. https://doi.org/10.1016/j.jbiotec.2016.01.031
45. Atencia J, Beebe DJ (2005) Controlled microfluidic interfaces. Nature 437(7059):648–655. https://doi.org/10.1038/nature04163
46. Hou S, Tiriac H, Sridharan BP et al (2018) Advanced development of primary pancreatic organoid tumor models for high-throughput phenotypic drug screening. SLAS Discov 23(6):574–584. https://doi.org/10.1177/2472555218766842
47. Shintaku H, Kuwabara T, Kawano S et al (2007) Micro cell encapsulation and its hydrogel-beads production using microfluidic device. Microsyst Technol 13(8–10):951–958. https://doi.org/10.1007/s00542-006-0291-z
48. Yue K, Trujillo-de Santiago G, Alvarez MM et al (2015) Synthesis, properties, and biomedical applications of gelatin methacryloyl (GelMA) hydrogels. Biomaterials 73:254–271. https://doi.org/10.1016/j.biomaterials.2015.08.045
49. Berkovitch Y, Yelin D, Seliktar D (2015) Photo-patterning PEG-based hydrogels for neuronal engineering. Eur Polym J 72:473–483. https://doi.org/10.1016/j.eurpolymj.2015.07.014
50. Benton JA, DeForest CA, Vivekanandan V et al (2009) Photocrosslinking of gelatin macromers to synthesize porous hydrogels that promote valvular interstitial cell function. Tissue Eng Pt A 15(11):3221–3230. https://doi.org/10.1089/ten.tea.2008.0545
51. Nichol JW, Koshy ST, Bae H et al (2010) Cell-laden microengineered gelatin methacrylate hydrogels. Biomaterials 31(21):5536–5544. https://doi.org/10.1016/j.biomaterials.2010.03.064
52. Fairbanks BD, Schwartz MP, Bowman CN et al (2009) Photoinitiated polymerization of PEG-diacrylate with lithium phenyl-2,4,6-trimethylbenzoylphosphinate: polymerization rate and cytocompatibility. Biomaterials 30(35):6702–6707. https://doi.org/10.1016/j.biomaterials.2009.08.055
53. Alessandri K, Feyeux M, Gurchenkov B et al (2016) A 3D printed microfluidic device for production of functionalized hydrogel microcapsules for culture and differentiation of human Neuronal Stem Cells (hNSC). Lab Chip 16(9):1593–1604. https://doi.org/10.1039/c6lc00133e
54. Carvalho MR, Barata D, Teixeira LM et al (2019) Colorectal tumor-on-a-chip system: a 3D tool for precision onco-nanomedicine. Sci Adv 5(5):1317. https://doi.org/10.1126/sciadv.aaw1317
55. Nguyen M, De Ninno A, Mencattini A et al (2018) Dissecting effects of anti-cancer drugs and cancer-associated fibroblasts by on-chip reconstitution of immunocompetent tumor microenvironments. Cell Rep 25(13):3884–3893. https://doi.org/10.1016/j.celrep.2018.12.015
56. Hassell BA, Goyal G, Lee E et al (2018) Human organ chip models recapitulate orthotopic lung cancer growth, therapeutic responses, and tumor dormancy in vitro. Cell Rep 23(12):3698. https://doi.org/10.1016/j.celrep.2018.06.028
57. Chen MB, Whisler JA, Frose J et al (2017) On-chip human microvasculature assay for visualization and quantification of tumor cell extravasation dynamics. Nat Protoc 12(5):865–880. https://doi.org/10.1038/nprot.2017.018
58. Shim S, Belanger MC, Harris AR et al (2019) Two-way communication between ex vivo tissues on a microfluidic chip: application to tumor-lymph node interaction. Lab Chip 19(6):1013–1026. https://doi.org/10.1039/c8lc00957k
59. Virumbrales-Munoz M, Livingston MK, Farooqui M et al (2019) Development of a microfluidic array to study drug response in breast cancer. Molecules 24(23):4385. https://doi.org/10.3390/molecules24234385
60. Virumbrales-Munoz M, Ayuso JM, Lacueva A et al (2019) Enabling cell recovery from 3D cell culture microfluidic devices for tumour microenvironment biomarker profiling. Sci Rep 9(1):6199. https://doi.org/10.1038/s41598-019-42529-8
61. Mannoor MS, Jiang ZW, James T et al (2013) 3D printed bionic ears. Nano Lett 13(6):2634–2639. https://doi.org/10.1021/nl4007744
62. Cui HT, Nowicki M, Fisher JP et al (2017) 3D bioprinting for organ regeneration. Adv Healthc Mater 6(1):1601118. https://doi.org/10.1002/adhm.201601118
63. Johnson BN, Lancaster KZ, Zhen G et al (2015) 3D printed anatomical nerve regeneration pathways. Adv Funct Mater 25(39):6205–6217. https://doi.org/10.1002/adfm.201501760
64. Zhang YS, Duchamp M, Oklu R et al (2016) Bioprinting the cancer microenvironment. ACS Biomater Sci Eng 2(10):1710–1721. https://doi.org/10.1021/acsbiomaterials.6b00246
65. Campbell A, Mohl JE, Gutierrez DA et al (2020) Thermal bioprinting causes ample alterations of expression of LUCAT1, IL6, CCL26, and NRN1L genes and massive phosphorylation of critical oncogenic drug resistance pathways in breast cancer cells. Front Bioeng Biotechnol 8:82. https://doi.org/10.3389/fbioe.2020.00082
66. Takagi D, Lin W, Matsumoto T et al (2019) High-precision three-dimensional inkjet technology for live cell bioprinting. Int J Bioprint 5(2):208
67. Kingsley DM, Roberge CL, Rudkouskaya A et al (2019) Laser-based 3D bioprinting for spatial and size control of tumor spheroids and embryoid bodies. Acta Biomater 95:357–370. https://doi.org/10.1016/j.actbio.2019.02.014
68. Koch L, Brandt O, Deiwick A, et al (2017) Laser assisted bioprinting at different wavelengths and pulse durations with a metal dynamic release layer a parametric study. Int J Bioprint 3(1): 001 https://doi.org/10.18063/ijb.2017.01.001
69. Keriquel V, Oliveira H, Remy M et al (2017) In situ printing of mesenchymal stromal cells, by laser-assisted bioprinting, for in vivo bone regeneration applications. Sci Rep 7(1):1778. https://doi.org/10.1038/s41598-017-01914-x
70. Zhao Y, Yao R, Ouyang LL et al (2014) Three-dimensional printing of Hela cells for cervical tumor model in vitro. Biofabrication. https://doi.org/10.1088/1758-5082/6/3/035001
71. Dai X, Liu L, Ouyang J et al (2017) Coaxial 3D bioprinting of self-assembled multicellular heterogeneous tumor fibers. Sci Rep 7(1):1457. https://doi.org/10.1038/s41598-017-01581-y
72. Schmidt SK, Schmid R, Arkudas A et al (2019) Tumor cells develop defined cellular phenotypes after 3D-bioprinting in different bioinks. Cells 8(10):1295. https://doi.org/10.3390/cells8101295
73. Grix T, Ruppelt A, Thomas A et al (2018) Bioprinting perfusion-enabled liver equivalents for advanced organ-on-a-chip applications. Genes (Basel) 9(4):176. https://doi.org/10.3390/genes9040176
74. Yu X, Zhang T, Li Y (2020) 3D printing and bioprinting nerve conduits for neural tissue engineering. Polymers (Basel) 12(8):1637. https://doi.org/10.3390/polym12081637
75. Alonzo M, AnilKumar S, Roman B et al (2019) 3D bioprinting of cardiac tissue and cardiac stem cell therapy. Transl Res 211:64–83. https://doi.org/10.1016/j.trsl.2019.04.004
76. De Pieri A, Byerley AM, Musumeci CR et al (2020) Electrospinning and 3D bioprinting for intervertebral disc tissue engineering. JOR Spine 3(4):e1117. https://doi.org/10.1002/jsp2.1117
77. Contreras-Caceres R, Cabeza L, Perazzoli G et al (2019) Electrospun nanofibers: recent applications in drug delivery and cancer therapy. Nanomaterials (Basel) 9(4):656. https://doi.org/10.3390/nano9040656

78. Kolesky DB, Homan KA, Skylar-Scott MA et al (2016) Three-dimensional bioprinting of thick vascularized tissues. PNAS 113(12):3179–3184. https://doi.org/10.1073/pnas.1521342113
79. Skardal A, Atala A (2015) Biomaterials for integration with 3-D bioprinting. Ann Biomed Eng 43(3):730–746. https://doi.org/10.1007/s10439-014-1207-1
80. Kyle S, Jessop ZM, Al-Sabah A et al (2017) 'Printability' of candidate biomaterials for extrusion based 3D printing: state-of-the-art. Adv Healthc Mater 6(16):1700264. https://doi.org/10.1002/adhm.201700264
81. Teixeira BN, Aprile P, Mendonca RH et al (2019) Evaluation of bone marrow stem cell response to PLA scaffolds manufactured by 3D printing and coated with polydopamine and type I collagen. J Biomed Mater Res B Appl Biomater 107(1):37–49. https://doi.org/10.1002/jbm.b.34093
82. Hu X, Man Y, Li W et al (2019) 3D bio-printing of CS/Gel/HA/Gr hybrid osteochondral scaffolds. Polymers (Basel) 11(10):1601. https://doi.org/10.3390/polym11101601
83. Florczyk SJ, Liu G, Kievit FM et al (2012) 3D porous chitosan-alginate scaffolds: a new matrix for studying prostate cancer cell-lymphocyte interactions in vitro. Adv Healthc Mater 1(5):590–599. https://doi.org/10.1002/adhm.201100054
84. Zhu W, Holmes B, Glazer RI et al (2016) 3D printed nanocomposite matrix for the study of breast cancer bone metastasis. Nanomedicine 12(1):69–79. https://doi.org/10.1016/j.nano.2015.09.010
85. Bernstein-Levi O, Ochbaum G, Bitton R (2016) The effect of covalently linked RGD peptide on the conformation of polysaccharides in aqueous solutions. Coll Surf B Biointerf 137:214–220. https://doi.org/10.1016/j.colsurfb.2015.06.042
86. Karel S, Sogorkova J, Hermannova M et al (2018) Stabilization of hyaluronan-based materials by peptide conjugation and its use as a cell-seeded scaffold in tissue engineering. Carbohydr Polym 201:300–307
87. Langer EM, Allen-Petersen BL, King SM et al (2019) Modeling tumor phenotypes in vitro with three-dimensional bioprinting. Cell Rep 26(3):608–623. https://doi.org/10.1016/j.celrep.2018.12.090
88. Elyada E, Bolisetty M, Laise P et al (2019) Cross-species single-cell analysis of pancreatic ductal adenocarcinoma reveals antigen-presenting cancer-associated fibroblasts. Cancer Discov 9(8):1102–1123. https://doi.org/10.1158/2159-8290.cd-19-0094
89. Mazzocchi A, Devarasetty M, Huntwork R et al (2018) Optimization of collagen type I-hyaluronan hybrid bioink for 3D bioprinted liver microenvironments. Biofabrication 11(1):015003. https://doi.org/10.1088/1758-5090/aae543
90. Miri AK, Nieto D, Iglesias L et al (2018) Microfluidics-enabled multimaterial maskless stereolithographic bioprinting. Adv Mater 30(27):e1800242. https://doi.org/10.1002/adma.201800242
91. Freeman S, Ramos R, Alexis Chando P et al (2019) A bioink blend for rotary 3D bioprinting tissue engineered small-diameter vascular constructs. Acta Biomater 95:152–164. https://doi.org/10.1016/j.actbio.2019.06.052
92. Murphy SV, Atala A (2014) 3D bioprinting of tissues and organs. Nat Biotechnol 32(8):773–785. https://doi.org/10.1038/nbt.2958
93. Parlato S, De Ninno A, Molfetta R et al (2017) 3D microfluidic model for evaluating immunotherapy efficacy by tracking dendritic cell behaviour toward tumor cells. Sci Rep 7(1):1093. https://doi.org/10.1038/s41598-017-01013-x